Flavin-dependent alcohol oxidase from the yeast *Pichia pinus*

Spatial localization of the coenzyme FAD in the protein structure: hot-tritium bombardment and ESR experiments

Alexander Z. AVERBAKH,*‡ Ninel D. PEKEL,† Vera I. SEREDENKO,† Alexander V. KULIKOV,* Rudolf I. GVOZDEV* and Inna P. RUDAKOVA†

*Institute of Chemical Physics, Russian Academy of Sciences, Institutsky str. 12, Chernoholovka, Moscow Region 142432, Russia, and †Research Institute of Vitamins, Nauchni str. 14a, Moscow 117820, Russia.

The spatial localization of the coenzyme FAD in the quaternary structure of the alcohol oxidase from the yeast *Pichia pinus* was studied by tritium planigraphy and ESR methods. In the present paper we measured the specific radioactivity of FAD labelled as a part of the alcohol oxidase complex. The specific-radioactivity ratio for two FAD portions (FMN and AMP) was calculated. ESR experiments show 4 Å (0.4 nm) to be the depth of immersion of paramagnetic isoalloxazines into alcohol oxidase octamer molecules. It is suggested that FAD molecules are bound to the surface of the octamer, rather than to the subunit interfaces. The orientation of the prosthetic group FAD in the alcohol oxidase protein is discussed.

INTRODUCTION

Flavin-dependent alcohol oxidase (AOX) is a key enzyme in methanol metabolism in yeasts, which converts methanol into formaldehyde and H_2O_2 [1–4]. An active form of the enzyme is an oligomer of about 670 kDa, consisting of eight identical subunits and containing eight FAD prosthetic groups [5]. In spite of recent success with crystallization of AOX [6–8], we do not yet have its structure at the atomic level. The enzyme is heterogeneous in its chromophore content: it contains approximately one-third of catalytically active oxidized FAD, the residual two-thirds consisting of approximately equal amounts of the anionic flavin radical and inactive oxidized flavin [1–3].

We investigated the spatial localization of the coenzyme FAD in AOX, using the hot-tritium bombardment and ESR techniques. Hot-tritium bombardment [9–11] is a relatively new technique that is useful for study of structure of protein surfaces. This method is based on high reactivity of tritium atoms produced via thermal dissociation of tritium molecules on a tungsten wire heated up to 2000 K. The depth of penetration of the reactive tritium atoms is 3–5 Å (0.3–0.5 nm) [12]. The tritium planigraphy method was used for study of accessible surfaces of many biological objects: purple-membrane bacteriorhodopsin [13], tobacco mosaic virus [14], *Escherichia coli* ribosomes [9,11] and pike parvalbumin III [15]. The ESR method of determining the immersion depth of radicals in macromolecules was proposed and tested experimentally in references [16–19]. The method is based on measurement of the effect of exogenously added and randomly distributed paramagnetic ions on the saturation curves of the radical's ESR spectra.

Here we report the values of specific radioactivity for FAD and for its two portions (AMP and FMN) isolated from AOX after the hot-tritium bombardment. We also evaluated the immersion depth of the paramagnetic isoalloxazines in the AOX octamers by the ESR method. The orientation of FAD molecules incorporated in the protein matrix is discussed.

MATERIALS AND METHODS

AOX from the methylotrophic yeast *Pichia pinus* was kindly given by Dr. E. R. Davidov (Russian State Institute 'Syntezbelok', Moscow). The specific activity of the enzyme (16–20 units/mg) was determined as described by Van der Klei et al. [20]. The protein concentration was determined as described in [21]. The AOX enzyme was subjected to hot-tritium bombardment in 3 ml samples at 14–18 mg/ml. The control samples (3 ml) used in this study include: (i) commercial FAD solution (Sigma, St. Louis, MO, U.S.A.), 300 μg/ml in 3 mM sodium phosphate buffer, pH 7.2; (ii) a mixture of 900 μg of FAD with 72 mg of BSA (fraction V; Boehringer, Heidelberg, Germany) in 3 mM sodium phosphate buffer; and (iii) a mixture of FAD with soybean trypsin inhibitor (STI). STI was purified from a crude STI preparation (Reanal, Budapest, Hungary) on a Mono Q HR 5/5 FPLC column (Pharmacia LKB, Uppsala, Sweden) developed with a linear 10–1000 mM gradient of NaCl. The STI-containing peak was eluted at 520 mM NaCl. Ultimately, the samples (3 ml) contained 40 mg of STI in 50 mM sodium phosphate buffer, pH 7.5, and 900 μg of FAD. The samples were frozen dropwise and were ground in liquid nitrogen. The bombardment procedure was performed as described [9,11].

The labelled samples were freeze-dried and the radioactivity of the water obtained was measured. The samples were dissolved in water (3 ml), incubated for 3 h and freeze-dried again. After eight cycles of freeze-drying, the samples were boiled for 3 min at 100 °C and 50 μl of 0.16 M $MgCl_2$ solution was added. The coagulated protein was sedimented at 12000 *g* for 20 min. The supernatant was incubated for 2 h and freeze-dried. Electrophoretic purification of the FAD samples was carried out with a 'Tabor OE 201' (Budapest, Hungary) apparatus for high-voltage electrophoresis by using Whatman 3MM paper, at 1300 V for 3.5 h in 0.05 M ammonium formate buffer, pH 5. The FAD spots were eluted in 6 ml of 4 mM sodium phosphate buffer and freeze-dried. Further chromatographic purification of the FAD samples were performed on Whatman 3MM paper in the pyridine/2-methylpropan-1-ol/water/acetic acid (33:33:33:1, by vol.) system for 15 h. Repeated ascending chromatography of FAD was performed on paper in aq. 5% (w/v) Na_2HPO_4 (pH adjusted to 7.8 with H_3PO_4). Finally, the FAD was eluted from the paper with 2.4 ml of 2 mM sodium phosphate buffer, and its radioactivity and concentration were determined as described [4].

The samples, containing 20–42 μg of FAD, were freeze-dried and dissolved in 4 ml of 0.1 M HCl. Then 3 mg of unlabelled FAD was added, and the pyrophosphate hydrolysis was carried

Abbreviations used: AOX, alcohol oxidase; STI, soybean trypsin inhibitor; FMN, flavin monophosphate.

‡ To whom correspondence should be addressed.

out for 1.5 h at 70 °C. The samples, adjusted to pH 3.5 with 0.5 M NaOH, were applied to a column (9 mm × 140 mm) of Spheron DEAE-1000 (Chemapol, Praha, Czech Republic), which had been equilibrated with acetate buffer, pH 3.5. Fractions of volume 10–70 ml were collected, dried and dissolved in 3 ml of water. Concentrations of AMP and FMN were determined by the absorbance changes at 259 nm ($\epsilon = 15.4 \times 10^3\ M^{-1} \cdot cm^{-1}$) and 445 nm ($\epsilon = 12.5 \times 10^3\ M^{-1} \cdot cm^{-1}$) respectively. Radioactivity was measured with a liquid-scintillation spectrometer 'Beta' (Kiev, Ukraine) in 2-ethoxyethanol/toluene scintillation mixture. The fluorescence spectra were taken with an Aminco–Bowman spectrophotofluorimeter (model J4-8963E; Silver Spring, MD, U.S.A.). The measurements were performed at 535 nm, with excitation at 448 nm. In all these samples, FAD concentration was 11 μM.

ESR spectra were recorded by a EPR-3 radiospectrometer (Novosibirsk, Russia) with modulation frequency of 20 kHz and a 600 mW klystron. The maximum strength of the microwave field in a H_{102} cavity, 0.93 G (0.093 mT) was determined by measuring microwave saturation of 1,1-diphenyl-2-picryl-hydrazyl, as described in [16]. The measurements were carried out at 77 K in a quartz dewar for AOX dissolved in water/glycerol mixture (1:1, v/v). The algorithm for determining spin-lattice relaxation time from parameters of saturation curves is described in [16,22]. Potassium ferricyanide was used as an exogenous paramagnet randomly distributed in the glassy solvent.

RESULTS

The radioactivity profiles obtained by the repeated chromatography of FAD labelled in a free state (a) or as a part of AOX (b) are shown in Figure 1. The background radioactivity did not exceed 46% of the total radioactivity in the eluted FAD spots. Table 1 displays data on specific radioactivity for FAD samples labelled under various conditions. The radioactivity was referred to that of the water obtained from the first freeze-drying. The standard value of the reference corresponds to a radioactivity of 7.3×10^7 Bq. Simultaneously, this procedure normalizes the magnitude of the tritium ampoule used, the target's geometrical features, and some inevitable variations of the bombardment regime.

Our values for FAD specific radioactivity (Ci/mg) are 10–100-fold lower than those obtained for amino acids and peptides [1,3,23]. This situation results from much lower contents of non-exchangeable hydrogen atoms in the FAD molecule. Compared with FAD labelled in the free state (Table 1), polypeptide chains of both AOX and BSA screened FAD molecules approx. 7- and 4-fold, respectively, whereas STI molecules had no shielding effect. The most reasonable explanation is that the FAD molecules are more or less buried in the polypeptide matrix of AOX and BSA, but not of STI. All systems discussed above were tested by FAD fluorescence measurements for BSA and STI solutions at the same concentrations. The data showed that the fluorescence intensity of the FAD/BSA mixture was 3 times lower than that for the FAD/STI mixture and approx. 35 times higher than that of AOX. The slopes of the Stern–Volmer plots of the FAD fluorescence quenching with KI in the range 20–160 mM of the FAD/STI and FAD/BSA systems coincide with the slope for the solution of free FAD, within 20% accuracy (approx. 30 M^{-1}). Accordingly, the apparent association constants for FAD/BSA and FAD/STI were $(1–2) \times 10^3\ M^{-1}$, as calculated from the concentration-dependency of the fluorescence (Klotz plots [24]). At the same time, our data demonstrate some quantitative differences between specific FAD binding to AOX and 'non-specific' binding to BSA (see Table 1). On the other hand, there are no qualitative differences.

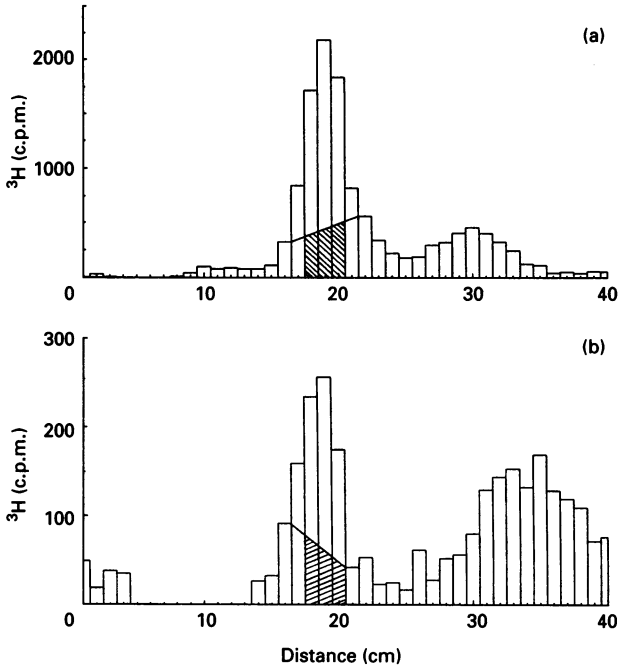

Figure 1 Distribution of the tritium label for the repeated chromatography of FAD obtained by heterogeneous counting in toluene scintillation mixture (typical experiments)

The paper strip of 8 mm width containing one of the spots was cut out perpendicularly to the chromatography front and then cut up into 5 mm pieces, which were deposited into the scintillation vials. (**a**) FAD labelled in free state; (**b**) FAD labelled as a part of AOX. The FAD spots were placed in sections 17–21 and 17–20, respectively, and the elution was performed from sections 18–20 for both (**a**) and (**b**). The hatched areas correspond to the background subtracted.

Table 1 Values of referred specific FAD radioactivity and specific-radioactivity ratio for the two FAD portions (FMN and AMP) labelled under various conditions

The specific radioactivity (A) of the dissolved substance is inversely proportional to the concentration to the power of $\frac{1}{3}$. The referred specific-radioactivity values of FAD isolated from AOX were standardized by division by the corresponding coefficient, ranging from 1.15 to 1.24. The root-mean-square deviations were calculated from three independent experiments, except that indicated by (*), which was obtained by averaging the data of two experiments.

	FAD labelled in free state	FAD labelled in mixture with BSA	FAD labelled in mixture with STI	FAD labelled as a part of AOX
Referred specific radioactivity (Ci/mol)	0.39 ± 0.06	0.093 ± 0.012	0.53 ± 0.22	0.056 ± 0.015
Specific-radioactivity ratio (A_{FMN}/A_{AMP})	9.0 ± 1.2*	4.0 ± 0.4	–	3.6 ± 0.7

The values of the specific-radioactivity ratio for two FAD portions (FMN and AMP), which are independent of any normalization coefficients, are summarized in Table 1. These values were calculated by using radioactivity profiles for the

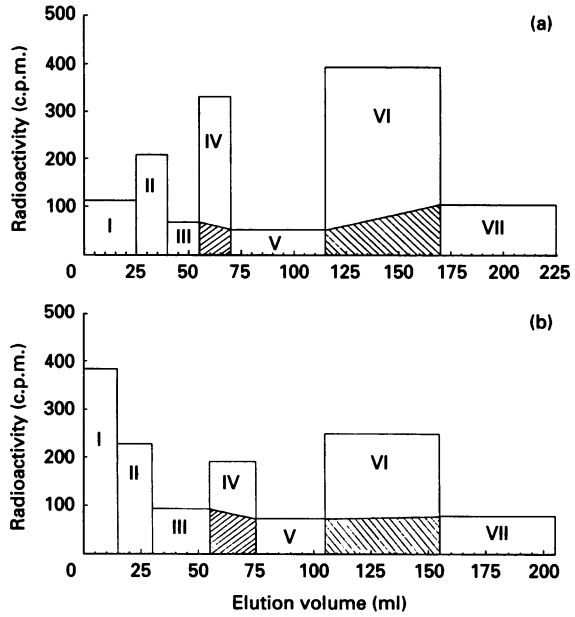

Figure 2 Profiles of the radioactivity distribution corresponding to the chromatographic separation of the FAD hydrolysates (typical experiments)

Samples for radioactivity counting (20 μl for fractions VI and VII, and 400 μl for the others) were taken from the specimens of volume 3 ml. The areas of the depicted columns correspond to the total radioactivity of the fractions. Fractions IV and VI contain AMP and FMN respectively. (**a**) FAD labelled in an equimolar mixture with BSA. (**b**) FAD labelled as a part of AOX. The hatched areas correspond to the background subtracted.

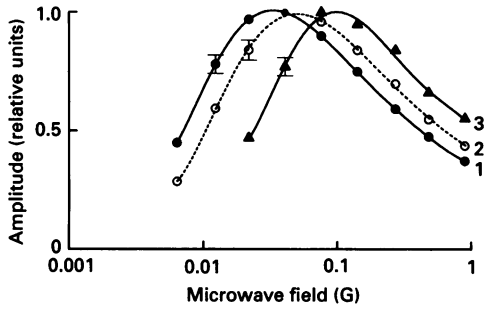

Figure 3 Saturation curves of ESR spectra of FAD in AOX at 77 K in a water/glycerol mixture at different concentrations of potassium ferricyanide: (1) 0; (2) 11 mM; (3) 120 mM

Error bars indicate the level of noise for the experiments.

corresponding chromatographic separations (typical examples are presented in Figure 2).

Figure 3 shows the saturation curves: a dependence of the amplitude (A) of the ESR line of AOX on strength of the microwave field (H_1). In the presence of ferricyanide ions, randomly distributed in the glassy solution, the saturation curve is shifted, due to the effect of magnetic dipole interaction on the spin-lattice relaxation time, T_1, of the FAD radicals [16–19]:

$$W \equiv \frac{1}{T_1} - \frac{1}{T_1^0} = \frac{\pi G(r_{min.}, R)\mu^2\gamma^2\tau C}{9r_{min.}^3} \quad (1)$$

where $r_{min.}$ is the distance of the closest approach of the ion and the radical, μ and τ are the magnetic moment and

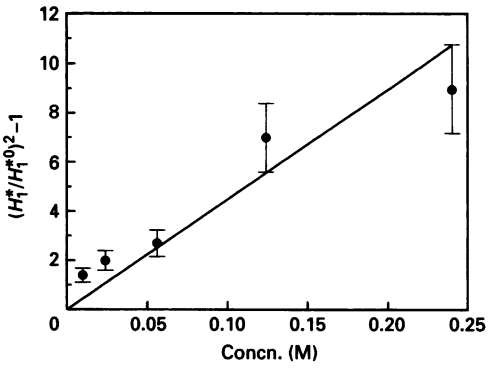

Figure 4 Dependence of $(H_1^*/H_1^{*0})^2 - 1$ on the concentrations of potassium ferricyanide

Error bars indicate root-mean-square uncertainties calculated from three independent experiments.

the spin-relaxation time of the ferricyanide ion, respectively ($\mu^2\tau = 1.0 \times 10^{-50}$ s·erg·G^{-1} [19]), γ is the gyromagnetic ratio for electrons, and C is the ion concentration. The geometric factor $G(r_{min.}, R)$ is a known function [17] of $r_{min.}$ and the radius of the AOX molecule, R. The index '0' denotes the value of T_1 at $C = 0$.

The values of T_1 can be determined by the algorithm proposed in [22] on the basis of the width of the ESR line, ΔH, and the parameters of the saturation curve, H_1^* and H_1^{**}, the strength of the microwave field at which the amplitude of the ESR line is equal to one-half of the maximum. For AOX at $C = 0$, $\Delta H = 1.38$ mT, $H_1^* = 0.73$ μT, $q = H_1^{**}/H_1^* = 50$, $T_1^0 = 2.8 \times 10^{-4}$ s. It is convenient to represent experimental data, by using the following formula [16–19]:

$$(H_1^*/H_1^{*0})^2 - 1 = T_1^0 W \quad (2)$$

The value of $(H_1^*/H_1^{*0})^2 - 1$ depends linearly on the concentration C (Figure 4), in accordance with eqn. (2). The ratio $W/C = 1.8 \times 10^5$ M^{-1}·s^{-1} can be determined from the slope of the straight line (Figure 4). This value is close to that for the free nitroxide radical in water/glycerol mixture (5.5×10^5 M^{-1}·s^{-1}) [16]. Evaluation of the immersion depth of paramagnetic isoalloxazines in the AOX octamer, $r = 0.4 \pm 0.2$ nm, can be made by solving eqn. (1) with respect to $r_{min.}$ [16–19], by using the W/C ratio given above and the value of $R = 6$ nm for the radius of the AOX octamer [5].

DISCUSSION

The selection of BSA as an object for the modelling of the non-specific FAD binding was based on the fact that serum albumins are proteins with a rugged flexible surface which binds a wide variety of compounds at more than one binding site [25–28]. The 'configurational adaptability' of BSA is due mainly to its structural features: BSA consists of three similar domains, each containing a hydrophobic slot [25–27]. Thus the equimolar mixture of FAD with BSA provided us with the required excess of binding sites. Gel-filtration chromatography of an equimolar mixture of FAD with BSA shows that approx. 76–81% of the added FAD is eluted together with BSA (Sephadex G-25 column 9 mm × 200 mm; elution with pure water). When STI was substituted for BSA, only 1–3% of the added FAD was eluted along with STI under the same conditions

(results not shown). The binding properties of BSA mentioned above are in good agreement with our data: for FAD/BSA mixture, the A_{FMN}/A_{AMP} ratio decreases by more than one-half (see Table 1). This phenomenon may reflect a particular orientation of the bound FAD molecule relative to the BSA polypeptide chain. The hydrophobicity of isoalloxazine substantially exceeds that of adenine. In the AMP non-exchangeable tritium atoms can be located at 2- and 8-positions in adenine and at the 5′-ribose carbon atoms, whereas the isoalloxazine moiety comprises eight strongly bound hydrogen atoms, six of which belong to the methyl groups. This feature may also explain the high value of the A_{FMN}/A_{AMP} ratio for FAD labelled in the free state.

The FAD molecules specifically bound to the AOX structure demonstrate a 7-fold decrease in accessibility to hot tritium atoms, as compared with FAD labelled in the free state. The AOX molecules appear as cube-like octamers (110 Å × 120 Å × 130 Å), consisting of two flat tetramers tightly packed together [5]. Electron microscopy of AOX two-dimensional crystals revealed that the tetramers are turned in relation to one another, and that adjacent subunits are connected by two narrow bridges [29]. The straightforward flow of tritium atoms could penetrate in exposed areas only [12,14,30], but not into the interfaces. For example, after the hot-tritium bombardment, approximately one-third of the 70 S ribosome proteins remain virtually unlabelled [9,11]. This is in good agreement with theoretical estimations carried out on the basis of the model of elastic collisions. For tritium atoms with the Maxwell distribution of velocities at 2000 K, the proportion of reactive atoms decreases to 3 % after passing through a layer of 3–5 Å (0.3–0.5 nm) width of the substance with the packing density corresponding to amino acid crystals [10]. The experiments performed with FAD mixed with double molar excess of STI could be used as a negative control for this technique. STI is widely known as a tightly packed and acidic protein (pI 4.6) [31]. Therefore phosphate residues in FAD and STI molecules will repel each other at pH 7.5. Thus it is not unexpected that STI molecules do not provide any detectable shielding for the FAD molecules. At the same time, the accessibility of FAD as a part of AOX does not differ qualitatively from that obtained for FAD mixed with BSA. The data obtained suggest that FAD molecules are bound to the surface of the AOX octamer rather than to the subunit interfaces. On the other hand, the FAD molecules could be positioned on the periphery of the interface. This possibility is strongly supported by ESR data: the calculated immersion depth of paramagnetic isoalloxazines into the octamer structure is about 4 Å (0.4 nm). Importantly, the saturation curves in the presence of potassium ferricyanide are shifted, but not broadened (Figure 3), i.e. the value of parameter q remains unchanged. This means that all paramagnetic FAD molecules are identical from the viewpoint of their location relative to the surface of the AOX octamer [16–19], i.e. the value of r for all paramagnetic isoalloxazines is the same.

The A_{FMN}/A_{AMP} radioactivity ratio obtained for the FAD isolated from AOX is significantly lower in comparison with FAD labelled in the free state. The riboflavin and adenosine portions of FAD are spatially separated by two phosphate residues which neither contain a tritium label nor contribute to measurements at all. Thus our data seem to reflect a particular orientation of FAD molecules with respect to the AOX protein surface, so that the riboflavin portion is buried deeper in the polypeptide than the adenosine (Table 1). At the same time, the riboflavin portion could be shielded to some degree by the adenosine moiety acting as an 'umbrella'. This suggestion is inconsistent with the generally accepted viewpoint, which states that the adenosine moiety is responsible for the FAD-binding affinity to the apoprotein [32,33]. This discrepancy might mean that the adenosine portion plays some other role in the yeast AOX.

Received 16 June 1994/9 May 1995; accepted 11 May 1995

REFERENCES

1 Sahm, H. and Wagner, F. (1973) Eur. J. Biochem. **36**, 250–256
2 Geissler, J. and Hemmerich, P. (1981) FEBS Lett. **126**, 152–156
3 Geissler, J., Ghisla, S. and Kroneck, P. M. H. (1986) Eur. J. Biochem. **160**, 93–100
4 Bystrykh, L. V., Dijkhuizen, L. and Harder, W. (1991) J. Gen. Microbiol. **137**, 2381–2386
5 Kato, N., Omori, Y., Tani, Y. and Ogata, K. (1976) Eur. J. Biochem. **64**, 341–350
6 Van der Klei, I. J., Lawson, C., Rozeboom, H., Dijkstra, B., Veenhuis, M., Harder, W. and Hol, W. G. J. (1989) FEBS Lett. **244**, 213–216
7 Boys, C. W. G., Hill, D. J., Stockley, P. G. and Woodward, J. R. (1989) J. Biol. Chem. **208**, 211–212
8 Tykarska, E., Lebioda, L., Marchut, E., Steczko, J. and Stec, B. (1990) J. Protein Chem. **9**, 83–86
9 Yusupov, M. M. and Spirin, A. S. (1986) FEBS Lett. **197**, 229–233
10 Volynskaya, A. V., Stripkin, A. Yu., Shishkov, A. V. and Goldansky, V. I. (1982) Dokl. Akad. Nauk SSSR **266**, 871–874
11 Yusupov, M. M. and Spirin, A. S. (1988) Methods Enzymol. **164**, 426–439
12 Goldansky, V. I., Rumyantsev, Yu. M., Shishkov, A. V., Baratova, L. A. and Belyanova, L. P. (1982) Mol. Biol. (Moscow) **16**, 528–534
13 Tsetlin, V. I., Alyonycheva, T. N., Shemyakin, V. V., Neiman, L. A. and Ivanov, V. T. (1988) Eur. J. Biochem. **178**, 123–129
14 Goldansky, V. I., Kashirin, I. A., Shishkov, A. V., Baratoava, L. A. and Grebenshchikov, N. I. (1988) J. Biol. Chem. **201**, 567–574
15 Gedrovich, A., Shishkov, A., Goldansky, V., Baratova, L., Grebenshchikov, N. and Efimov, A. (1991) Eur. Biophys. J. **19**, 283–286
16 Kulikov, A. V., Cherepanova, E. S. and Bogatyrenko, V. R. (1981) Teor. Eksp. Khim. **17**, 787–795
17 Kulikov, A. V., Cherepanova, E. S., Bogatyrenko, V. R., Nasonova, T. A., Fisher, V. R. and Yakubov, Kh. M. (1987) Izv. Akad. Nauk ASSR, Ser. Biol. **5**, 762–769
18 Likhtenstein, G. I., Kulikov, A. V., Kotelnikov, A. I. and Levchenko, L. A. (1986) J. Biochem. Biophys. Methods **12**, 1–28
19 Likhtenstein, G. I., Kulikov, A. V. and Kotelnikov, A. I. (1992) in Bioactive Spin Labels (Zhdanov, R. I., ed), pp. 181–200, Springer-Verlag, Berlin and Heidelberg
20 Van der Klei, I. J., Bystrykh, L. V. and Harder, W. (1990) Methods Enzymol. **188**, 420–427
21 Kalb, V. F. and Bernlohr, R. W. (1977) Anal. Biochem. **82**, 362–371
22 Safronov, S. N., Mstislavskii, V. I., Safronova, U. I. and Muromtsev, V. I. (1969) Zavod. Lab. **35**, 1463–1468
23 Kolb, V. A., Kommer, A. A. and Spirin, A. S. (1987) Dokl. Akad. Nauk. SSSR **296**, 1497–1501
24 Klotz, I. (1947) Chem. Rev. **41**, 373–375
25 Peters, T., Jr. and Reed, R. G. (1977) Albumin: Struct. Biosynth., Funct.: Proc. FEBS Meet. **50**, 4–17
26 Wilton, D. C. (1990) Biochem. J. **270**, 163–166
27 Carter, D. C., He, X. M., Munson, S. H., Twigg, P. D., Gernert, K. M., Broom, M. B. and Miller, T. Y. (1989) Science **244**, 1195–1198
28 Johanson, K. O., Wetlaufer, D. B., Reed, R. G. and Peters, T. (1981) J. Biol. Chem. **256**, 445–450
29 Vonck, J. and van Bruggen, E. F. J. (1990) Biochim. Biophys. Acta **1038**, 74–79
30 Ivlev, A. B., Gedrovich, A. V. and Shishkov, A. V. (1992) Mol. Biol. (Moscow) **26**, 1047–1053
31 Birk, Y. (1985) Int. J. Pept. Protein Res. **25**, 113–131
32 Dixon, M. (1971) Biochim. Biophys. Acta **226**, 241–258, 259–274
33 Tsuge, H. and Mitsuda, H. (1974) J. Biochem. (Tokyo) **75**, 399–406